Hydrogen transport in amorphous silicon

W. B. Jackson and C. C. Tsai

Xerox Palo Alto Research Center, 3333 Coyote Hill Road, Palo Alto, California 94304
(Received 24 July 1991)

The diffusive transport of hydrogen is used to investigate H trapping in hydrogen-depleted amorphous Si (a-Si) samples and to determine a rough H-diffusion density of states. The diffusion profiles show clear evidence of deep traps separated from shallow traps, and the results are well explained by a simple division of the H states into deep traps, shallow traps, and transport states. The concentration of deep traps is about $(0.8-2) \times 10^{20}$ cm^{-3}, of which about 30% can be identified with dangling bonds. The energy of the deep traps is at least 1.9 eV below the transport states. The diffusion is dispersive with a power-law time dependence and can be characterized by an exponential distribution of hopping barriers with a width of roughly 0.09 eV. The shallow traps are identified with clustered H pairs which determine the H chemical potential at high H concentrations. The results are compared with calculations and other recent ideas on H bonding energetics. The results are consistent with a range of possibilities. One extreme is the case in which H is predominately bonded on void surfaces and the transport energy is substantially different in a-Si than in crystalline Si (c-Si); the other extreme is the case in which H predominately resides in platelet structures and the transport energy is roughly the same as in c-Si. The actual case depends on the deposition conditions.

I. INTRODUCTION

Hydrogen bonding and transport are important for understanding the structure, growth, and metastability of amorphous silicon. Because of the diffusion and evolution of high concentrations of hydrogen during growth, the structure of hydrogenated amorphous silicon (a-Si:H) reflects the kinetics of hydrogen trapping (bonding) and detrapping (bond breaking). Configurations acting as deep traps will tend to be more stable and predominate over those configurations acting as shallower traps. Furthermore any Si configurations in a-Si:H must be relatively stable in the presence of large interstitial H fluxes. In this picture, highly strained bonds, for example, are expected to be less prevalent in films with significant H concentrations than in films without H. Despite the importance of understanding H bonding in a-Si:H, H bonding and transport remain poorly understood. The purpose of this paper is to apply H transport measurements, analogous to electron time-of-flight and charge collection measurements, combined with other structural probes to identify H trapping configurations in a-Si:H.

Hydrogen bonding and transport has been studied for a number of years primarily through diffusion and evolution measurements. Early diffusion transport measurements have found that H diffuses with an activation energy of about 1.5 eV.[1-3] Structural measurements have identified several different hydrogen phases in a-Si:H. From infrared absorption measurements, H has been found to be predominately bonded in Si-H bonds characterized by 2000 and 2100 cm^{-1} vibration bands.[4,5] The 2100-cm^{-1} line is attributed to Si-H bonds on the surface of voids[6-8] and if associated with modes at 840–880 cm^{-1}, due to (Si-H$_2$) and (Si-H$_2$)$_n$ polysilane configurations.[4,5] The 2000-cm^{-1} vibration is less certain but is believed to be due to Si-H bonds located within the bulk.[4,5] Nuclear magnetic resonance (NMR) further supports the two-phase model for H. One component responsible for the narrow line is due to H comparatively isolated from the nearest-neighbor H on the order of 0.43 nm or larger while a second clustered phase is characterized by an inter-H distance on the order of 0.23 nm or larger.[9-11] H evolution experiments have shown that the isolated Si-H configurations represent deeper binding sites than the clustered and polyhydride configurations.[2,12,13]

Detailed measurements of the Si dangling-bond electron spin density as a function of annealing indicate that most of the H cannot be bonded in simple isolated Si-H bond sites since the total spin density following H elimination or before posthydrogenation is usually 100–1000 times lower than the concentration of bonded H. The comprehensive hydrogen evolution studies of Refs. 12–14 indicate that most of the increase in dangling-bond density occurs upon evolution of the most deeply bound H—presumably associated with the isolated H configurations. Zellama et al. suggested that the isolated H is more strongly bound than the weakly bound H. Disorder of course causes considerable variation in the energies of the various H configurations.

One promising way of dealing with the complexity of the various bonding configurations is to consider H bonding in terms of a density of states. As for electrons, specific microscopic configurations exhibit a range of positions causing a distribution of energies which can be represented by a density of states.[15] Bonding in a given configuration is equivalent to occupancy of the state. The barriers to configuration changes are equated with the energy required to reach a transport energy. The hydrogen chemical potential μ_H separates the occupied and

unoccupied states. Implicit in the utility of the density-of-states concept for transport is the assumption that H changes its configuration only by becoming interstitial at an energy E_c. Diffusion by a pair of H, for example, is assumed to be negligible. The energies of the various configurations are defined in terms of transition energies to and from the interstitial transport level. Using the density-of-states picture various aspect of hydrogen bonding, defect densities, and film structure have been understood.

One such model, using the idea of a negative effective correlation energy (U) for H, has had success in explaining the dependence of the dangling-bond density on H content and temperature.[15-17] This model extends previous work by identifying the weakly bound clustered H phase with two H configurations such that the binding energy of the second H $[E_c - E_{H_2^*(1/2)}]$ is greater than the first $[E_c - E_{H_2^*(0/1)}]$—a property resulting in pairing of the H [Fig. 1(a)]. The Si dangling bonds occur either from H transferred from the isolated configuration to the paired configuration, a small singly occupied fraction of the paired configurations, or a combination of both these factors. The first possibility has been investigated in detail in Refs. 16 and 17. In this work, single energy levels for the isolated H (E_{SiH}), paired configurations $[E_{av} = (E_{0/1} + E_{1/2})/2]$, and the correlation energy ($U = E_{1/2} - E_{0/1}$) have been invoked to account for the temperature dependence of the spin density. The 0.3-eV activation energy for the spin density of high H concentration material is due to a 0.3 eV $= \mu_H - E_{SiH} = E_{av} - E_{SiH}$ separation between the iso-
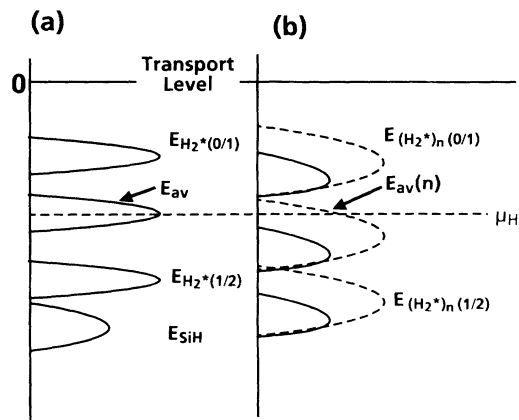
(a)   **(b)**

FIG. 1. H transition density of states from various configurations to the interstitial transport level for (a) 1H and 2H configurations and (b) multi-H configurations. E_{SiH} is the energy for an isolated Si-H bond. $E_{(H_2^*)_n(1/2)}$ and $E_{(H_2^*)_n(1/2)}$, $n = 1$ to the largest cluster, are the 0H to 1H and 1H to 2H transition levels for configurations consisting of n H_2^* pairs. $E_{av}(n) = (E_{(H_2^*)_n(0/1)} + E_{(H_2^*)_n(1/2)})/2$. The largest clusters are most stable and grow at the expense of clusters smaller than a critical size. The dashed lines in (b) indicate the range of possible energies for $n = 1$ at the top to n large at the bottom while the solid lines indicate schematically those platelets which actually exist.

lated H energy level and the average energy level of the paired phase. The equilibrium defects N_s are due to unoccupied SiH, $N_s \simeq N_{SiH} \exp[-(\mu_H - E_{SiH})/kT]$. As the hydrogen concentration is decreased, the number of paired H configurations decrease, μ_H becomes unpinned by the negative U defects at E_{av} and decreases to the isolated H energy level E_{SiH}. The spin activation energy decreases to a small value.[16,17]

A variation of this model is that for high hydrogen concentrations, the spins can arise from singly occupied clustered configurations in addition to unoccupied isolated sites.[18,19] For most cases with substantial H content, the defects in a-Si:H are assumed to arise primarily from single occupancy of the clustered configurations rather than unoccupied isolated dangling-bond defects. In this case the 0.3-eV activation energy, approximately equal to $E_{H_2^*(0/1)} - E_{av} = U/2$ for a single level, is not due a small $U = 0.6$ eV but rather due to the additional assumption that the disorder results in a distribution of paired energies ($E_{av}, E_{H_2^*(0/1)}$ and $E_{H_2^*(1/2)}$). The distribution of the $E_{H_2(0/1)}$ energies reduces the effective spin activation energy $E_{H_2(0/1)} - \mu_H$. The isolated H configurations are roughly 0.5–1.2 eV below μ_H determined by the clustered H. μ_H resides in a minimum of the H density of states pinned by E_{av}. Only in the H depleted cases do the unoccupied isolated H configurations contribute significantly to the spin concentration since μ_H becomes pinned by E_{SiH}. Thus, the energy difference between μ_H and the Si-H bonding level is critical in determining whether the thermal equilibrium spins arise from single occupancy of multiple H states or unoccupied isolated dangling bonds.

The previously mentioned models have dealt primarily with energetics and thermodynamics of defect densities and H trapping. Recent theoretical[20-28] and experimental[28] progress in understanding H-bonding configurations in crystalline Si suggest new possibilities for microscopic identification of the various H phases in a-Si:H. According to local-density pseudopotential calculations, H bonding to an isolated dangling bond is indeed a low-energy configuration -2 to -2.5 eV below both the interstitial bond-centered H, H(BC), and the interstitital H in the T_d site, H(T_d).[21-23,26] Theory therefore predicts that isolated dangling bonds should be the deepest traps for H. The most interesting development has been the discovery that H prefers to form pairs and clustered configurations even in c-Si.[22] In the case of H pair formation, one H occupying a bond-centered position of a Si-Si bond breaks the Si-Si bond. The remaining dangling bond is passivated by H occupying the antibonding site forming another somewhat weaker Si-H bond. This paired configuration, denoted by H_2^*, is calculated to be about -0.75 eV/H atom lower in energy than for isolated interstitial H atoms.[22,23] The energy varies with the strength and distortion of the Si-Si bond at the H_2^* location. The defects arise from dissociation of paired H to form singly occupied configurations responsible for the observed spin density.[19,23] Metastability occurs when carriers cause dissociation of paired H by capture of one or both types of carriers.[25] The H_2^* is therefore a prime candidate for the

negative-U H configuration.

Unfortunately the situation is more complex. Both theory[23] and experiments[28-30] in the hydrogenation of c-Si show that at high H concentrations, H forms even larger H configurations consisting of many clustered H. These H_2^* pairs form larger n hydrogen plateletlike clusters denoted by $(H_2^*)_n$ oriented along a local Si$\langle 111 \rangle$ direction in c-Si.[23,29,30] The same clustering and pairing mechanisms apply to amorphous silicon as well since the configurational energies do not depend on long-range order but rather on the local bonding configurations which are nearly the same on average between c-Si and a-Si. The clustered H phases detected in NMR and IR may be identified with the platelet structures in a-Si:H—similar to c-Si H platelets. The NMR linewidth is consistent as well as the energies.[31] Neturon scattering shows the existence of hydrogen with an approximately 12-nm radius of gyration.[32,33] Thus, at high concentrations, H is believed to form various-sized clusters in Si. The energy of these clusters depends on cluster size, n in addition to variations due to disorder [Fig 1(b)]. These discoveries have further implications on the density of states which will be discussed in this paper.

Despite this progress, much remains uncertain regarding H bonding in a-Si. In particular, the energies of H bound in an isolated dangling-bond relative mobile interstitial H is unknown. Theoretical calculations estimate the difference to be as large as 2.5 eV (Refs. 12 and 26), while some a-Si models assume that this energy is on the order of 1.5–1.8 eV.[15] Also the position of μ_H pinned by the clustered H phase relative to Si dangling bonds is not known experimentally. One model assumes that it is about 0.3 eV while calculations indicate that the energy difference between H platelets and isolated Si-H could be as large as 1.2 eV.[12,26] In fact, general energetic arguments as well as specific calculations for H on Si(110) indicate that the energy of H trapping ranges over at least half a Si-Si bond energy or about 1.2 eV.[27] Moreover, the location of the mobile H transport level in a-Si:H may be different from that found in c-Si due to the presence of extended arrays of strained bonds and low-energy pathways for H diffusion further complicating identification of microscopic models for H bonding in a-Si:H. Summarizing, one would like to determine the H trapping density of states analogous to the electronic density of states determined for a-Si:H, and if possible identify the microscopic configurations responsible for the various states.

In the case of the electronic density of states, electronic transport and charge collection experiments were invaluable for determining the number and energy distribution of electronic states.[34-36] The drift mobility for electrons is dominated by trapping into various states depending on the time, temperature, and other conditions of transport. The activation energy of the mobility under a given configuration indicates the depth of the traps controlling the transport for that particular situation. In a similar fashion, in this work, H transport measurements, analogous to time-of-flight measurements, are used in this work to determine trapping properties and the number and energy location of H states within the material. Al-

though the motion of H is diffusive, the effect of trapping is quite similar to the case of transport by drift. The basic idea is to measure the diffusive transport of H in the presence of H traps. In the case of charge carriers, the time dependence of the charge centroid is measured as a function of time via charge induced in the external electrode. Because the time scales for H transport are so vastly different, H transport measurements can be performed by diffusing H or D into the material and observing the spatial profile directly at a fixed time with secondary-ion mass spectroscopy (SIMS). When the H concentration is less than the density of traps, the H falls into deep traps and the diffusion is dominated by thermal emission from the deep traps. Once the traps are filled, diffusion is dominated by trapping and release from shallower traps. Measurements of H transport as a function of time and temperature permit estimation of the number and depth of the traps controlling transport for a given situation. Correlations between SIMS, IR, Raman, and electron spin resonance (ESR) permit a determination of the H-bonding configurations responsible for various features in the H density of states. The results of this study are used to assemble a tentative H density of states with the incorporation of possible ideas of the microscopic identification of various features.

II. EXPERIMENT

The experimental methods used to determine H trapping density of states relies on well-established methods of SIMS analysis in samples exposed to atomic H or D. The H content and therefore the trap occupancy are controlled both through evolution and posthydrogenation. One of the unique features of this study is that H-depleted samples are used.

A. Samples

Of fundamental importance for understanding transport in a-Si is the necessity of samples with a controllable number of traps which do not exhibit irreversible thermal changes under conditions necessary for H or D diffusion. Since diffusion occurs in temperature ranges of 250–450 °C for time periods of up to 2 h, the samples must be stable for these temperatures. Furthermore, traps must be unoccupied in order to trap H. The samples should also be stable with respect to exposure to air in order that the diffusion step can be separated in time and location from the SIMS analysis. These requirements are best met by H-depleted samples fabricated in the following manner. Glow discharge material produced under standard conditions is deposited at a substrate temperature of 350 °C on large 10 cm $\times$ 10 cm Cr covered 7059 substrates. The H content was around 8 atm. %. These samples, between 200- and 350-nm thick, are subjected to a series of increasing temperatures for longer times as given in Table I in order to drive the H out of the sample with a minimum of bubble and crack formation. The gas within the furnace during annealing consisted of pure N_2 with less than 10 ppb O_2 and other impurities. The samples spent a total of 9 h above 500 °C

TABLE I. Sample annealing schedule for producing H-depleted samples.

Temp. (°C)	Time (h)
350	1
400	4
450	3
475	3
500	3
525	3
550	3
ramp down	3

reducing the H content to below 1×10^{20} cm^{-3}. Raman scattering indicated that no crystallization resulted from this extended treatment at high temperatures. Following the high-temperature annealing, this large sample was cut into small 0.5 cm $\times$ 1.0 cm samples. The small samples exhibited spin variations of on the order of 10% or less thus demonstrating that the starting material is quite uniform.

The posthydrogenation procedure of the small samples consisted of the following steps. Prior to hydrogenation, the samples were given a metal-oxide-semiconductor (MOS)–grade detergent cleaning, a deionized water rinse, a 40-s dip in a 20:1 HF water mixture, and a second deionized water rinse, and were dried using filtered dry N$_2$. These steps, standard in c-Si MOS technology, remove any oxide which might have formed because of the high-temperature annealing. The spin density was measured before and after oxide removal and did not show any change. The samples were exposed to an optically isolated, remote atomic H or D plasma for various time periods ranging from 5 min to 2.5 h. The microwave power was held to 70 mW at 2.1 GHz. The gas pressure was 2 Torr and the D flow rate was about 9 SCCM (SCCM denotes cubic centimeter per minute at STP). The concentration of atomic H (or D) above the sample was estimated to be about 10^{15} cm^{-3} using ESR measurements of atomic H in a nearly identical plasma.[37] Most often D was used since the dynamic range for SIMS detection of D is much greater than that for H. Little difference was detected between H and D, however. In the rest of this paper, hydrogenation and deuteration will be considered more or less equivalent. The sample temperature was controlled by contact to a water-cooled temperature-controlled copper block. The H or D plasma was ignited when the sample reached the appropriate temperature for 5 min and was terminated after the sample had been rapidly cooled (10 °C/s to 150 °C) in order to keep any highly mobile H species within the film. The H or D concentration was controlled by inserting a stainless-steel mesh in the path between H generation in the plasma and the sample and by increasing the distance by up to 6.5 cm between the plasma and the sample. This allowed more atomic H to recombine to form H$_2$ molecules reducing the flux of H perhaps by as much as a factor of 100.

B. Measurements

A number of measurements were made on the samples to determine various properties of the films. The primary measurement consisted of SIMS measurements made with a Cameca using a Cs beam. Typical depth resolutions obtained for these runs are 7.5–9.0 nm per factor of e of concentration change, although a few runs may have resolutions as poor as 12.5 nm. Both H and D were measured in most of the samples. For a few samples, O, C, and N profiles were obtained. The O, C, and N existed only at the surface and did not diffuse any detectable distance into the dehydrogenated film even following a six-month exposure to air. Thus, the H-depleted, anneal-stable samples resist oxidation unlike evaporated a-Si films.

Raman measurements were measured before and after hydrogenation to discern the effect of hydrogenation on the structure. These results, discussed in greater detail in Ref. 38, can be summarized as follows. The H enters the sample predominately in a Si-H configuration characterized by a 2000-cm^{-1} vibration frequency. The amplitude of the Si-H vibration roughly corresponds to the SIMS measurement of the concentration indicating that the bulk of the H is apparently bonding to Si rather than forming H$_2$ molecules. There is no detectable narrowing of the Si transverse-optic phonon peak. The width of this peak is proportional to the rms bond-angle disorder. In fact, the peak actually broadens on the high-frequency side as would occur if a small number of Si bonds were subjected to compressive stress. The $\sim$7 at. % H apparently does not decrease Si bond-angle disorder but rather increases it slightly. To first order, H does not significantly decrease the number of strained Si-Si bonds.

The spin-density measurements were made at room temperature. Before high-temperature annealing the spin density was $(1-3) \times 10^{16}$ cm^{-3}. After annealing, the spin density ranged from $(2-3) \times 10^{19}$ cm^{-3} for the unhydrogenated films to about 2×10^{17} cm^{-3} for the material exposed to long periods of hydrogenation at high temperatures. In a previous study,[39] the spins of some of these samples were spatially profiled by cycles of sequential etching followed by total spin measurements. On companion samples, the deuterium concentration was also profiled; the results are shown below. Hence the relation between the spin-density profiles and D could be determined.

Finally, on some samples photothermal deflection spectroscopy (PDS) measurements of the effect of hydrogenation was made. The films showed a marked reduction of the subgap absorption but little change in the Urbach-edge region—results consistent with the Raman measurements also indicating little change in the number of weak bonds. Because of the short diffusion distance interference fringes dominate the spectra, making these measurement of limited use.

III. RESULTS

The deuteration was performed at a number of different temperatures and times. Typical D SIMS re-

sults are shown in Fig. 2 for three different temperatures at fixed times. A least-squares fit of the high-concentration data to a complementary error function of the form $H_f(0)\,\mathrm{erfc}[x/(4D_{\mathrm{eff}}t)^{1/2}]$ where $H_f(0)$ is the concentration at the surface x is the distance into the film, D_{eff} is the effective diffusion coefficient, and t is the diffusion time is indicated by the dashed line. From these results it is apparent that for high concentrations greater than $(8-9)\times10^{19}$ cm^{-3}, the transport can be characterized by a single diffusion coefficient. Below $(8-9)\times10^{19}$ cm^{-3}, the profiles become sharp exponential curves whose slope is probably limited by the spatial resolution of SIMS. As will be discussed below, this behavior is exactly what one would expect from diffusion in the presence of deep traps. An interesting feature of the data is that the deviation from a complementary error function occurs near the concentration of H remaining within the film Another point of interest is that the surface concentration decreases as the hydrogenation temperature increases.

In Fig. 3, the D concentration profiles for two different temperatures (solid points) are superimposed on the measurements of the spin profiles (squares) along with the results of simulations of trapping dominated diffusion discussed below (solid lines). Note that the spin density decreases markedly when the D concentration exceeds the resulting density of dangling bonds. The spin density is within a factor of 3–4 of the concentration at which the profile deviates from a complementary error function.

For each time and temperature, the high-concentration regions of the SIMS profiles could be fit to a complementary error function yielding $H_f(0)$ and D_{eff} as a function of the time and temperature of deuteration. The results are shown in Figs. 4 and 5. The diffusion coefficient in Fig. 4 depends rather strongly on temperature and also somewhat on time consistent with previous measurements.[40–42] Hence the activation energy, roughly 1.1–1.3 eV, is only approximately correct because of the time dependence of the diffusion coefficient. The time

dependence becomes more pronounced as the temperature decreases, as expected from multiple trapping. This result indicates that there is a distribution of hopping times for H as it diffuses through the network. Because the time dependence varies with temperature, the distribution of hopping times is likely to arise from distributions of energies for H trapping sites. Hence information about H trapping densities of states is contained in the time and temperature dependence of D_{eff}.

The surface concentration exhibits little systematic change with time (Fig. 5) but increases significantly as the temperature is lowered particularly below 400 °C. The lack of any observable time dependence supports the idea that the Si network structure is roughly independent of H concentration at these temperatures. If the Si network were undergoing major irreversible changes in response to the presence of H, the equilibrium concentration of H would change as the Si network readjusted. Since this is not observed, we conclude that anneal-stable Si network is approximately stable for H or D incorporation at the temperature and times necessary to diffuse H. The rate at which H arrives at the surface is more or less independent of the sample temperature, but the rate at which H atoms diffuse toward each other within the sample to form H$_2$ and leave the film, and the rate at which H overcomes barriers to leave the film, increase strongly with

FIG. 3. The deuterium concentrations (dots) vs the normalized sample distance (sample thickness is 300 nm) for two different temperatures and spins profiled as in Ref. 39 (squares) under conditions as in Fig. 2. The solid lines represent solutions to trap limited diffusion equations.
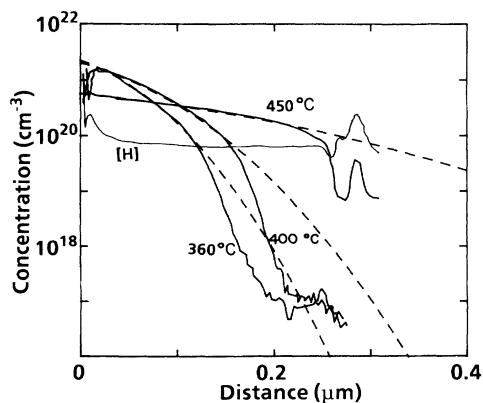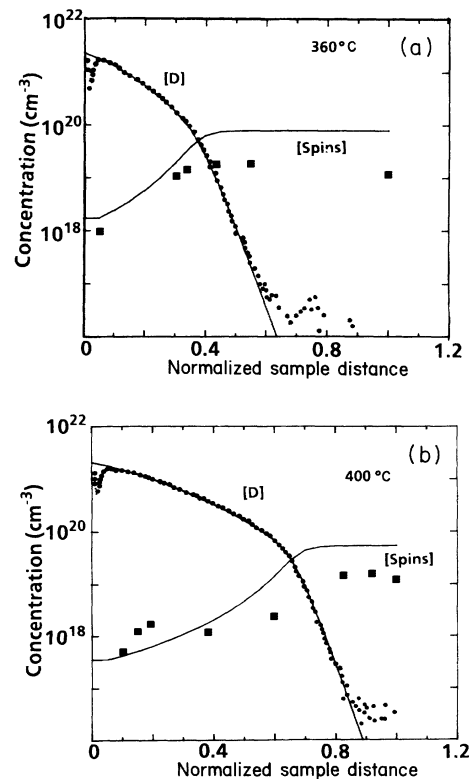

FIG. 2. Deuterium concentration vs distance for exposure to atomic D at the indicated temperatures (solid) and the H concentration in a sample without D exposure. The dashed lines depict a least-squares fit to an erfc form. Diffusion times are 30, 25, and 90 min for 360, 400, and 450 °C, respectively.
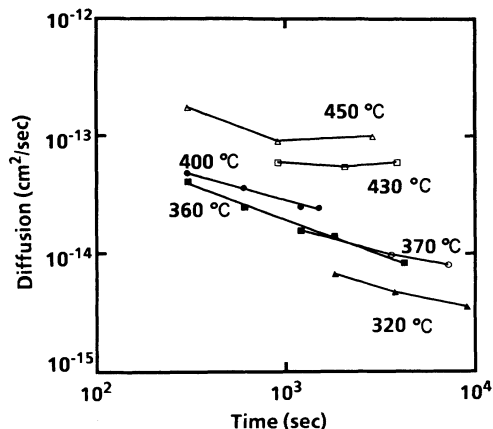
FIG. 4. The effective shallow-trap dominated diffusion coefficient vs time for the indicated temperatures. The time dependence increases as the temperature decreases.

FIG. 6. Deuterium concentration vs distance for attenuated D exposures at various indicated temperatures and times. For concentrations below 8×10^{20} cm^{-3} little diffusion is observed.

temperature. Since the concentration is determined by a balance between the incoming and departing H, the surface concentration decreases as the temperature is increased. $H_f(0)$ averaged over time is activated with an activation energy of about 0.65 eV as shown in Fig. 5. This value gives some idea of the barrier for H to leave the sample but a precise determination depends on the order of the reaction as well. This is substantially less than the 1.9-eV surface barrier for H evolution in the absence of atomic H.[43]

The SIMS data in Figs. 2 and 3 indicate that for concentrations below about 10^{20} cm^{-3}, the diffusion coefficient is significantly lower than for D concentrations above 10^{20} cm^{-3}. Hence if the concentration of D is reduced below 10^{20} cm^{-3}, the diffusion coefficient should be substantially smaller. In Fig. 6, the D profiles for samples exposed to a D flux attenuated by passing the atomic
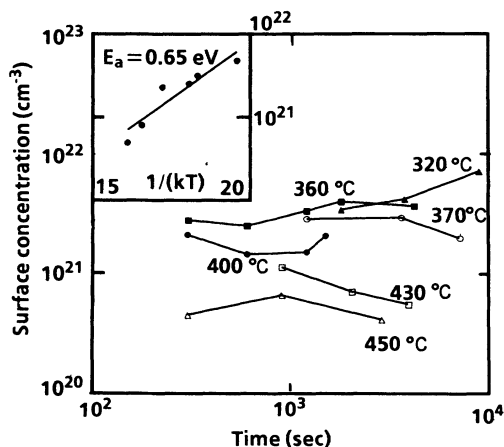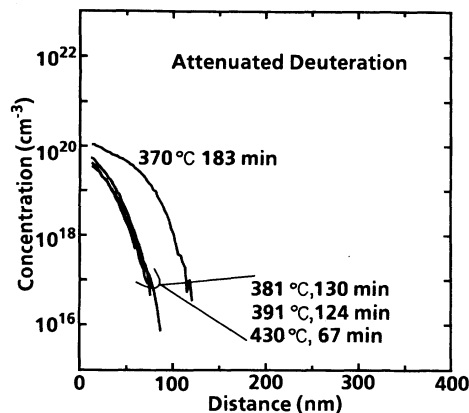

FIG. 5. The surface average concentration vs time for the indicated temperatures. The inset shows the surface concentration (H per cm^3) averaged over time vs $1/kT$. The effective activation energy is 0.65 eV but there is not much change below 400 °C.

D through a stainless-steel mesh and increasing the path to the sample by the insertion of a 5-cm-long stainless-steel flange are depicted. For the higher temperatures of 381, 391, and 430 °C the concentration was held slightly below the 10^{20}-cm^{-3} density of traps so the diffusion was significantly reduced. For the 370 °C data, the concentration exceeded the trap density, and the diffusion increased dramatically despite being at a lower temperature. The dominant portion of the attenuated D curves for the higher temperatures is an exponential characteristic of the SIMS resolution (8.0-nm broadening). The curvature in the first 30 nm is due to the fact that the concentrations are only slightly below the trap density of 10^{20} cm^{-3} so a small fraction of the H diffuses in the shallower states. The absence of any temperature dependence indicates that there is virtually no D diffusion within the SIMS resolution distance of 8 nm for temperatures as high as 430 °C and times as long as 67 min. Hence, the diffusion coefficient can be estimated at less than about $(8 \times 10^{-7}$ cm$)^2/(4 \times 4020$ s$) = 4 \times 10^{-17}$ cm^2/s even at 430 °C. These data establish a minimum depth of traps responsible for D trapping as discussed below.

Finally, the introduction of D has a remarkable effect on the H concentration. In Fig. 7, the D and H concentration of films subjected to the indicated deuteration conditions are shown. D causes a depletion of the H in regions of high-D concentration and a buildup of H near the leading edge of the D where it exceeds the H concentration and the trap density. This dislodging of H increases for longer times. Ultimately, H is induced to leave the sample resulting in a reduced H concentration. This occurs at times and temperatures significantly lower than those used to anneal the sample. Hence, D lowers the barrier to remove H from the sample. These observations are consistent with results of Abeles et al. (Ref. 44) who observed that D displaces H in superlattices and Ref. 45 indicating that atomic D can reduce the H content in a film. These observations indicate that trapped H can be released during the diffusion experiment in the high-D region where the traps are occupied and diffuse to other regions of the sample.
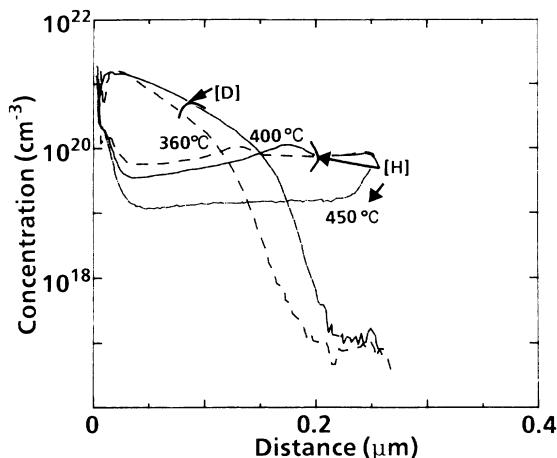
FIG. 7. D and H concentrations vs distance for 360 °C (dashed line), 400 °C (top solid line), and 450 °C (lower solid line). The 450 °C D was left off because the D extended throughout the film. This exposure to D significantly reduced the H content. In all cases of diffusion through only part of the film, the H concentration peaked near the leading edge of the D profile.

IV. DISCUSSION

In general, the transport of H through amorphous Si is a highly complex process depending on the H concentration, time, temperature, and the state of the silicon network, as well as the density of H traps. Despite this complexity, simplifying assumptions may be made to understand the overall features of H transport in the H-depleted material. It is particularly useful to adopt many of the concepts and principles developed for electron transport to understand H transport keeping in mind that there are significant differences.

A. H diffusion in a-Si

1. Simplifying assumptions for H transport

H diffuses into a-Si by a series of thermally activated hops between positions in the Si network. The Si network may also readjust to a limited extent in response to the presence of the H. If the Si network changes irreversibly due to the trapping of H such that the possible H configurations are significantly different after the H leaves a region than before it arrived, then the concept of the H density of states is of limited utility. Fortunately, because the presence of H during growth eliminates vacancies, interstitials, and other mobile point defects and the relatively low temperatures below 450 °C used during diffusion, negligible Si diffusion is expected to take place. For example, the self-diffusion coefficient of Si of 20 cm²/s exp[(−4.77 eV/kT)] which means that the extrapolated Si diffusion coefficient at 450 °C is around 4×10^{-30} cm²/s or at most, Si atoms change positions at a rate of 1.4×10^9 cm⁻³s⁻¹ assuming a mean hopping distance of 0.25 nm. Thus even after hours, few Si atoms attempt to change places in c-Si at these temperatures. Furthermore, the Si network has been subjected to an ex-

tended anneal for many hours reaching temperatures of 550 °C. Hence, this network is expected to be relatively stable against irreversible thermally induced reconstructions at lower temperatures. If the diffusion or transport experiments occur at temperatures higher than the highest anneal temperature, the network may exhibit irreversible changes and interpretation of transport becomes more complex.

In this case when the Si network retains its overall structure, various positions within the Si network can be regarded as states which can trap H, and the concept of a H density of states is useful. H bonding and debonding in a given configuration is then expressed as H capture and release from the trap representing that configuration. The number of H atoms which can trap at these sites can vary from 1 to a large number, and in general multiple-H clusters can form. Due to entropic considerations, the 1H and 2H configurations predominate at lower concentrations, while the multiple H_2^* clusters prevail at higher concentrations. The 1H and 2H configurations are best treated as multioccupancy sites as described in Fig. 1(a). The transition energies (actually the Gibbs free energies) associated with an extended cluster of H pairs are best treated according to nucleation and growth theory. The large $(H_2^*)_n$ clusters of paired H have lower average H binding energies $E_{av}(n)$ than smaller clusters, and tend to grow at the expense of smaller clusters. The number of H traps associated with the larger clusters increase while those associated with smaller ones decrease. The growth of the lower-energy large clusters tends also to pin μ_H near $E_{av}(n)$ in a small density of transition levels (states) consistent with Ref. 46.

H is expected to move primarily as a monatomic species executing random hops from site to site, although in some void rich material, molecular H_2 transport is believed to occur.[13] Both the barriers between sites and the site energies will exhibit a distribution characteristic of or related to the Si network disorder. Unlike the case of electrons, tunneling is not expected to be important, and the transport energy E_C will not be the same even for nearby sites. Thus, transport probably does not take place at a limited range of energies near a mobility edge but rather through an extended range of energies—a range perhaps even as large or larger than the distribution of trap energies. Furthermore, the number of sites available to a H excited to the top of a barrier is limited to a small number (2–4) whose release barriers are likely to be strongly correlated with the previous barrier. This is in contrast to electron transport where once an electron is excited to the mobility edge it has numerous possible new traps to sample, and the release rate from the new trap is uncorrelated with that of the previous trap. Finally, in the case of H transport, the number of H atoms is significant compared to the number of sites, so trap filling and H-H interactions may be important.

With these differences between electron and H transport in mind, we nevertheless can adapt many concepts used for electron transport to understand H-diffusion results. We assume that there is an effective 1H density of states which approximates effects the multihydrogen densities of states in quasiequilibrium with transport states.

These states can be approximately divided into three groups on the basis of their energy. (i) The highest-energy states are transport states representing the tops of barriers between various sites. The transport states are located in a range around E_c. (ii) Shallow trapping states are located below these transport states and come to equilibrium with the transport states during the diffusion experiments. (iii) Finally the lowest-energy states are deep trapping states which do not reach equilibrium with the mobile H during the experiment. The energy dividing the shallow and deep states E_d depends on the time scale and temperature of the experiment[46] and is approximately given by

$$E_d = E_c - kT \ln(\omega t) , \qquad (1)$$

where T is the temperature of the experiment, t is the time, and ω is the attempt frequency of about 10^{12}–10^{13} Hz. The situation easiest to analyze occurs when this energy roughly lies in a region of reduced densities of states permitting a relatively clean separation between the two types of trapping states.

Following electron dispersive transport, we assume the transport of monatomic H in the transport states is characterized on average by a "microscopic" diffusion coefficient D_{micro} which is more or less independent of temperature or H concentration. The transport due to trapping and release from the shallow traps over various barriers is characterized by an effective diffusion coefficient D_{eff} which is a function of the distribution of H within the shallow states and therefore is a function of time and H concentration. The deep traps are characterized by their capture coefficient $K = 4\pi R_c D_{\text{eff}}$,[47] where R_c is the trap capture radius, the release rate is ν, and the trap density is N_T. ν is temperature activated with an activation energy equal to the depth of the trap below E_c. In general, we find that lumping all deep traps together into a single effective trap is sufficient to explain the data. Also it is assumed that the diffusion experiments occur at sufficiently low temperatures and short times that the free hydrogen does not reach equilibrium with the various large clusters.

Under these assumptions, the concentration of H diffused into a sample is governed by the combined diffusion and trapping equations,

$$\frac{\partial H_f}{\partial t} = D_{\text{eff}} \frac{\partial^2 H_f}{\partial x^2} - K H_f (N_T - H_t) + \nu H_t , \qquad (2)$$

$$\frac{\partial H_t}{\partial t} = K H_f (N_T - H_t) - \nu H_t , \qquad (3)$$

where H_f and H_t are the concentrations of "free" H in the transport and shallow states and deep-trapped H, respectively. The boundary condition is $H_f(0) = \text{const}$. If $H_f(0) \gg N_t$ then the traps are not important, and the diffusion characterized by the standard form

$$H_f = H_f(0)\,\text{erfc}(x/\sqrt{4D_{\text{eff}}t}) , \qquad (4)$$

where erfc is the complementary error function.

If $H_f < N_t$ and $\nu/(KN_T) < 1$, then the diffusion is trap dominated and the concentration profile becomes ex-

ponential of the form[48,49]

$$H_t = N_T \exp(-x'/x_0) , \qquad (5)$$

where x' is the distance beyond point where $H_f \simeq N_t$, and the decay length x_0 is approximately given by

$$x_0 = (4\pi R_c N_T)^{-1/2} \left[1 + \frac{\nu}{KN_T} \right]^{1/2} . \qquad (6)$$

If the deep-trapping states are well separated in energy from the shallow traps, then there will be a sharp division between the erfc and exponential dependence when the concentration equals N_T. The concentration at which the profile deviates from an erfc behavior is approximately equal to N_T. If ν is small compared to KN_T, x_0 is independent of temperature and can be used to determine the capture radius since N_T is known.

If the surface concentration $H_f(0)$ is less than N_T, then for sufficiently long times such that $E_d < E_t$ where E_t is the energy of the deep traps the functional form of the concentration returns to an erfc form. The deep-trap dominated effective drift diffusion D_{eff} dominated by N_T traps at E_T becomes

$$D_{\text{eff}} = D_{\text{micro}} \frac{n_c}{n_c + n_T} , \qquad (7)$$

$$D_{\text{eff}} \simeq D_{\text{micro}} (N_c/N_T)$$
$$\times \exp[-(E_c - \mu_H)/kT] \quad \text{for } E_T < \mu_H \qquad (8)$$

or

$$D_{\text{eff}} \simeq D_{\text{micro}} (N_c/N_T)$$
$$\times \exp[-(E_c - E_T)/kT] \quad \text{for } E_T > \mu_H , \qquad (9)$$

where D_{micro} is the microscopic diffusion in the transport states, n_c and n_T are the densities of H in the transport states and deep-trapped H, respectively, and N_c and N_T are the total number of transport states and deep-trapped levels, respectively. In Eqs. (7)–(9) the H trapped in shallow traps is neglected since the total H concentration is less than N_T.

2. Deep H traps

Equations (2) and (3) can readily be solved by finite difference techniques using explicit and Crank-Nicolson methods to test Eqs. (4)–(6) and compared to experimental curves. The boundary conditions are assumed to be a constant $H_f(0)$ at the surface and 0 at the back surface. The initial H_f and H_t concentrations are 0 throughout the film. The solid lines in Figs. 3(a) and 3(b) represent the total H concentration $H_{\text{tot}}(x) = H_f(x) + H_t(x)$ as a function of distance and the concentration of unoccupied traps $N_T - H_t(x)$. The agreement is quite good for the D concentrations and reasonable for the spin concentration. In such a comparison to the spin densities, we are assuming that each trap is a Si dangling bond when unoccupied. Of course this need not be the case since void surfaces contain weak reconstructed bonds which act as deep H traps and yet do not possess a spin. Other than

the magnitude, there is good agreement on the overall spatial dependence as well as the time dependence between the unoccupied traps and the spin density. The assumptions leading up to Eqs. (2)–(6) seem to be well verified by the data. In particular there appears to be an effective H density of states which is approximately independent of temperature or time during the experiment suggesting that the Si network is more or less fixed. In this density of states the H deep-trapping states are well removed from the shallow-trapping states as indicated by the sharp transition between the erfc and exponential spatial dependence.

The agreement between experiment and theory allows us to extract properties of the deep traps from the data with some degree of confidence. We find that for several series of runs that the number of deep traps is about 1×10^{20} cm^{-3} including the states occupied by H independent of the temperature or time of the experiment. The close agreement between the spatial dependence of the spin density and the empty trap population suggests that at least 25% of the traps in H-depleted material are in fact isolated dangling bonds. Since the error on the spin-density profiles is about a factor of 3–4, a majority of the deep traps may in fact be isolated dangling bonds. Interestingly, this number of traps (0.2 at. %) is almost identical to the density of traps found for Pd diffusing through unhydrogenated a-Si produced by self-implantation in c-Si relaxed by a long high-temperature thermal anneal.[50] Hydrogen can also release Pd from these traps. This suggests the possibility that the defects responsible for deep trapping in both forms of unhydrogenated Si (H-evolved glow discharge and implantation) may be independent of the sample preparation method. This result lends support to the idea in Ref. 50 that there are intrinsic defects in an "ideal" relaxed amorphous Si whose quasiequilibrium concentrations may be determined by thermodynamic equilibrium rather than by previous sample history.

In principle, we can determine the capture radius from Eq. (6) and v from the temperature dependence of x_0. Unfortunately, this exponential slope is due to the SIMS spatial resolution, rather than trapping. The SIMS resolution is typically 7.7–8.5 nm determined from the slope of the C signal arising from surface carbon contamination. As a result the actual slope of the D profile for concentrations below 8×10^{19} cm^{-3} is much steeper than that measured by SIMS. The fact that the low concentration diffusion profiles in Fig. 6 do not depend on temperature indicates that there is no trap emission during these diffusion experiments. Since the microscopic diffusion, weighted by trap density ratios, is on the order of 10^{-2} cm^2/s (see discussion below) and the diffusion coefficient is less than 4×10^{-17} cm^2/s at 430 °C, from Eq. (8) the traps must be at least 1.9 eV or more below the average transport energy. A similar conclusion can be obtained from the requirement that $v/(KN_T) \ll 1$ in order to see the kink in the concentration profile. Assuming that the density of levels at the transport energy is about 10^{22} cm^{-3} and using detailed balance, this relation requires that traps be at least 0.3 eV below the states controlling diffusion to see the kink at 430 °C. We can also place a

lower bound on the capture radius using Eq. (6) since $x_0 < (4\pi N_T R_C)^{-1/2}$ with $N_T = 10^{20}$ cm^{-3} and $x_0 = 8.0$ nm giving $R_c > 0.012$ nm. This limit is not particularly enlightening since one would expect that the capture radius is likely to be about 0.2 nm, the size of a dangling bond.

According to the assumption that sharp exponential edges in the concentration profiles are due to deep trapping, we would expect that hydrogenation prior to exposure to D should reduce the number of deep traps. We exposed samples to 420 °C, 2.5 h of hydrogenation at two different atomic H concentrations. The lower concentration was obtained by inserting a stainless-steel mesh between the plasma and the sample to serve as a recombination surface for atomic H. The H concentration for the unattenuated (attenuated) hydrogenation was roughly 16 (4) times greater than a hydrogen-depleted sample (Fig. 8). Two sets of three samples, where each set consisted of two hydrogenated samples at different H concentrations plus an unhydrogenated sample, were exposed to D at 340 and 382 °C. The resulting D and H concentration profiles for the 382 °C exposure are shown in Fig. 8. The most heavily hydrogenated sample exhibits the most rounded D profile and the largest $x_0 = 13.7$ nm. The spin density after hydrogenation for this sample was 2.5×10^{17} cm^{-3}. The attenuated hydrogenated sample had a spin density of 1.9×10^{18} cm^{-3} and $x_0 = 10.4$ nm. Finally, the fully H-depleted sample exhibited the sharpest kink due to extensive deep traps. The spin density for this sample was 2.1×10^{19} cm^{-3} and $x_0 = 8.1$ nm. The increasing value of x_0 is expected from Eq. (6) as the density of deep traps is reduced by trap filling. The magnitude of the increase in x_0 and the trap density, determined by the point of deviation from an erfc form, are smaller than one would expect from Eq. (6) if spins were the only traps. We would expect that x_0 should increase by a factor of
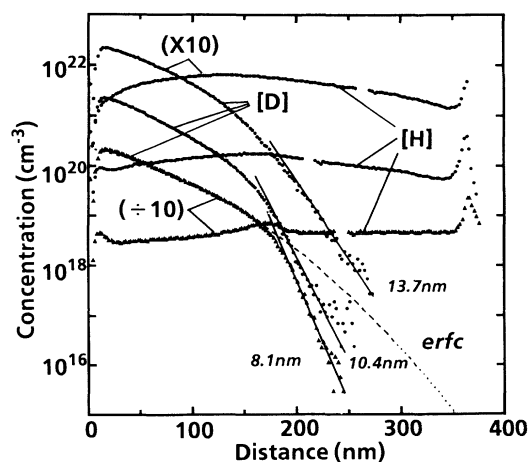

FIG. 8. Deuterium concentration (points) vs distance for three samples with varying concentrations of H (points) offset for clarity. The dashed line represents a least-squares error function and the solid lines indicate the change in slope as the prehydrogenation fills traps, reducing their trapping effect. The exponential slopes are indicated.

$\sqrt{10} \simeq 3$ instead of the observed factor of 1.3 comparing the attenuated hydrogenation sample to the heavily hydrogenated sample. Some of this difference may arise from the fact that for the lower H films, the slope is determined by SIMS resolution masking the true change in x_0. Furthermore, the kink concentration does not seem to decrease, indicating the possibility that some shallower traps are associated with H—an effect to be analyzed in a future publication. Nevertheless, the fundamental effect is observed that hydrogenation removes the traps and has the expected rounding effect on the profile. This result provides further confirmation that deep trapping is responsible for the exponential tail of the diffusion profile.

3. H detrapping

We turn our attention to the intriguing curves of Fig. 7 showing that D displaces H. This effect can readily be explained in terms of the deep-trap shallow-trap model. Because D and H compete for the same deep traps, a large concentration of D raises μ_H increasing the concentration of mobile H. As a consequence, H diffuses to regions of low-D concentration where it gets trapped. The H profile can be generated by expanding Eqs. (2) and (3) to keep track of trapped and free H and D separately according to the relations

$$\frac{\partial H_f}{\partial t} = D_{\text{eff}} \frac{\partial^2 H_f}{\partial x^2} - KH_f(N_T - D_t - H_t) + vH_t \qquad (10)$$

and

$$\frac{\partial H_t}{\partial t} = KH_f(N_T - D_t - H_t) - vH_t \qquad (11)$$

and two similar equations where H_t and H_f are replaced by D_t and D_f, respectively. These four equations can also be solved as Eqs. (2) and (3). The solid lines in Fig. 9 depict the total D concentration $D(x) = D_t(x) + D_f(x)$, the total H concentration, and the unoccupied deep traps given by $N_T - D_t(x) - H_t(x)$ plotted along with the H, D, and spin profiles. The calculated H concentration ex-
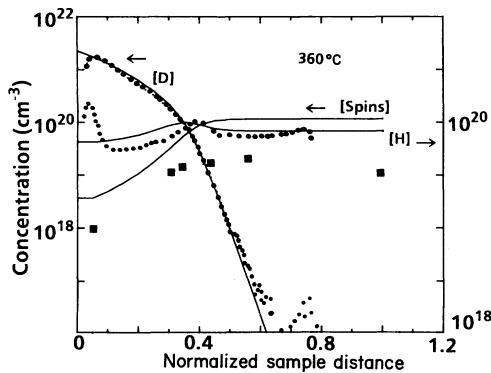

FIG. 9. The H, D (dots), and spin (squares) concentrations for 360 °C from Figs. 2 and 8 vs normalized sample thickness. The solid lines depict the calculated profiles assuming that H and D compete for the same traps.

hibits the same peak near the leading edge of the D profile and depletion behind as observed in the data. The H peak due to surface H present in the data is of course neglected in the calculation. The precise fit depends on the various trapping and diffusion parameters for H and D and can be made quite close to the data assuming various reasonable parameters. The purpose of the simulation here is to provide further evidence that the observed H transport in H-depleted a-Si can be well represented by a simple model which divides the states into three types: mobility states, shallow traps, and deep traps.

These data also may help place limits on the depth of the traps occupied by H relative to the transport levels. In order for this effect to be observed, the barrier to release must be small enough to occur during the diffusion experiment. Assuming a simple thermal release and an attempt frequency equal to the Si-H vibration frequency, it cannot be released from traps deeper than about 2.4 eV. However, this conclusion assumes that thermal release is the dominant method for H to leave traps. In the presence of interstitial H and D, another possibility exists: exchange of the interstitial and trapped H without fully breaking the Si-H bond.[44] Such an effect is believed to cause the enhanced evolution of H in the presence of D as seen in Fig. 7 and Ref. 51. If this possibility occurs the H traps could be even deeper than 2.4 eV.

4. Shallow H traps

When the concentration exceeds the density of deep traps, D_{eff} provides us with information about the energy depth and distribution of the shallow traps. The time dependence of D_{eff} (Fig. 4) indicates that there is a distribution of hopping times associated with H motion in the shallow traps. Since D_{eff} is strongly dependent on temperature, the distribution of hopping times is most likely related to a distribution of hopping energy barriers and therefore, the dispersion characteristics should also exhibit a temperature dependence. In the usual view of electron or hole multiple trapping excited by optical excitation, the decrease of the transport coefficients arises from the carrier population gradually occupying deeper energy states as time progresses. The same process may apply during posthydrogenation. H near the surface could be excited and then relax into deeper states as time progresses. Alternatively, the dispersion may arise from an approximately exponential distribution of barriers to hopping arising from either distributions of transport energy barriers, distributions of initial starting energies, and/or changes in H occupation and multiple H configurations as hydrogenation proceeds. Regardless of the precise microscopic model, the time dependence of D_{eff} can be analyzed in terms of a hopping time distribution. If this hopping time distribution arises from an approximately exponential distribution of energy barriers characterized by an energy width kT_0, then the time dependence is approximately given by

$$D_{\text{eff}}(t) = D_{\text{micro}}(wt)^{-\alpha} = D_{\text{micro}}(wt)^{-(1-\beta)} , \qquad (12)$$

where ω is an attempt frequency, $\beta = T/T_0$, and T is the measurement temperature.

There is clearly a general decrease in the slope of the data as the temperature decreases, which can be seen in the data in Fig. 4. This marked change of slope with diffusion temperature is not expected from a H-tunneling model which would predict temperature-independent transport, and thus confirms assumptions made earlier. In Fig. 10, the dispersion parameter β is plotted versus T. The solid line gives the behavior expected for $T_0 = 1074$ K, a value near the anneal temperature of 823 K characterizing the disorder of the silicon network. While the data in Fig. 10 are not of sufficient quality to prove unequivocally that β is linearly proportional to the temperature, they are clearly consistent with this possibility and are consistent with other work.[41-43] It should be pointed out that if the energetic distribution of barriers is not exactly exponential, the dispersion parameters will not lie on a line intercepting (0,0).[52] Nevertheless, the dispersion can be interpreted in terms of an approximate exponential distribution of barriers for hopping between shallow traps. This result is of interest because it indicates that the shallow traps are distributed in energy.

The temperature dependence of D_{eff} provides important information about energy depth of the shallow states in the H density of states. The energy difference between μ_H, the trap energy, and the transport energy can be estimated from the activation energy of D_{eff} according to Eq. (9) assuming that there is no peak in the occupied H states above μ_H. While dispersion introduces some uncertainty in the measurement of the activation energy, the activation energy for the diffusion over a fixed distance is roughly 1.0–1.3 eV—a value close to the 1.4–1.5 eV observed for hydrogenated a-Si:H. Thus, the important result from this section is that the shallow traps are located roughly 1.5 eV below the transport level and that this energy is approximately the same for H-depleted samples and as-grown samples. This activation energy is significantly larger than the 0.3–0.5 eV reported in Ref. 51. However in this latter case, substantial etching occurred during the posthydrogenation treatment indicating different H concentrations and ions due to the plasma. The diffusion is highly sensitive to these factors.

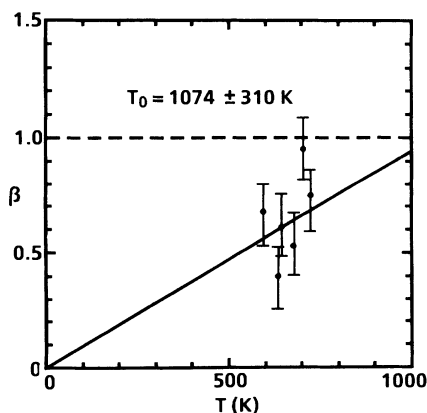Summarizing the H density-of-states information de-

rived thus far, the deep traps are at least 1.9 eV below the transport level with a concentration of 10^{20} cm^{-3}. The shallow traps are about 1.3–1.5 eV below the transport level with concentrations of at least 4×10^{21} cm^{-3}. There is a distribution of energies for release from the shallow traps giving rise to a distribution of release times which depends on temperature.

B. Determination of changes in trap depths

In this section, further information about the energies and microscopic models for states responsible for the various H density-of-states features in a-Si identified in the previous sections is presented. This goal is accomplished by comparing experimental H-diffusion results in c-Si to those in a-Si. From this comparison we get a prescription for determining trap energies that avoids problems arising from the strong concentration dependence. Furthermore, a unified picture for transport in both crystalline and amorphous Si emerges. These results are then used to identify various traps for H and develop possible microscopic models accounting for H transport in a-Si.

The idea developed in this section is that the energy of H diffusion changes when the traps controlling diffusion change providing the possibility of trap identification on the basis of energy. Equations (8) and (9) indicate that the activation energy of the diffusion is related either to the controlling traps or to μ_H. In particular, if the diffusion in a material without traps is compared to the diffusion in the same material with traps as in Fig. 11(a), the diffusion without traps will have an activation energy characteristic of the energy to hop to neighboring sites.
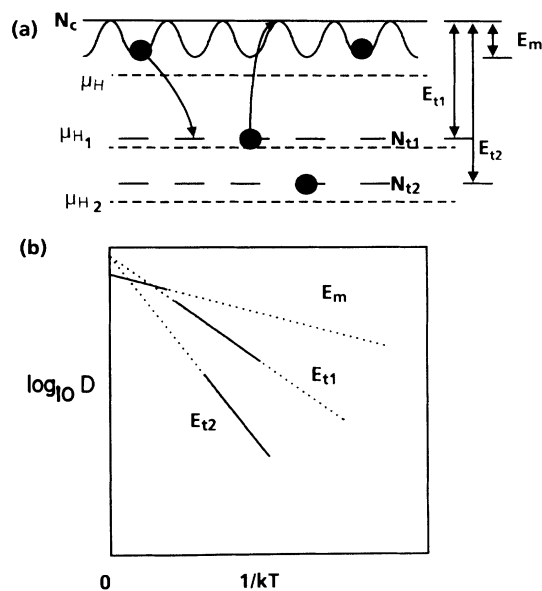

FIG. 11. (a) presents the effect of traps on diffusion. E_m is the diffusion activation energy without traps, while E_{t1} and E_{t2} are traps of different energy and concentration N_{t1} and N_{t2}. μ_H is the position of the chemical potential assuming that the traps outnumber the H atoms. (b) indicates the resulting plot of log$D$ vs $1/kT$.

FIG. 10. Dispersion parameter β vs temperature from the diffusion time dependence in Fig. 3.

If deep traps predominate, the activation energy will increase. Thus, a significant change in the diffusion activation energy is indicative of a change in the nature of the traps controlling diffusion as characterized by their energy.

Unfortunately, because diffusion can be greatly affected by statistical shifts and changes in concentration with temperatures, the activation energy can be difficult to determine accurately. This problem is graphically illustrated in Fig. 6 where a *negative* trap depth would be derived using the standard activation analysis. A similar problem has been encountered in the study of conductivity in a-Si:H, where it was found that activation energies were more reliable determined by assuming a prefactor and then deriving the appropriate activation energy.[53] We propose that a similar procedure be applied for H diffusion as well. The prefactor $(N_c/N_T)D_{micro}$ consists of the microscopic diffusion coefficient and the ratio of densities of states—typically a factor of 100 or less [Eq. (9)]. Hence, a plot of $\ln D_{eff}$ versus $1/kT$ should show that the diffusion data for a family of samples with different types of traps lie on different lines intercepting the $1/(kT)=0$ line at the same prefactor within a factor of 100 or so [Fig. 11(b)]. The depth of the trap can be determined by assuming the prefactor and determining the appropriate activation energy. Summarizing, we propose that by plotting D_{eff} versus $1/kT$ for a variety of different samples, those films which lie on significantly different activation curves have traps of different energy and therefore probably have different microscopic origins. This procedure for identifying changes in traps and trap energies is verified first by considering c-Si, and is then applied to a-Si.

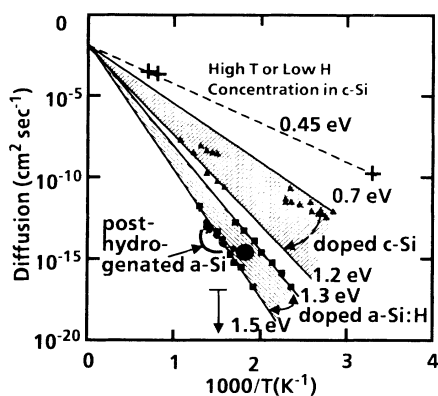A summary of diffusion data versus temperature for a variety of c-Si and a-Si samples is presented in Fig. 12. The diffusion at low concentrations and/or high temperatures in c-Si shows an activation energy of 0.45 eV (crosses and dashed line).[48,54] Equation (9) and Fig. 11(a) show that the transport level in c-Si is about 0.45 eV above the average interstitial site. The $(kT)^{-1}=0$ intercept gives $D_{micro} \simeq 10^{-2}-10^{-3} cm^2 s^{-1}$ assuming that the number of barrier states and interstitial sites are comparable. This is a reasonable number since $D_{micro}=(\frac{1}{6})va^2=10^{-3}-10^{-2} cm^2 s^{-1}$ for an attempt frequency v of 10^{13} Hz and a hopping distance a of 0.3–0.6 nm. The activation energy increases when traps are added. It is well established now that B acceptors and P donors act as traps for H diffusion in c-Si.[28] Hence, the addition of dopant traps changes the activation energy line that the diffusion data lies on as represented by the triangles in Fig. 12. The activation energy changes due to the varying concentrations of dopants and diffusion H as well as the effects of the Fermi-level position. Nevertheless, many series of data from single experiments in doped c-Si have an intercept near $10^{-3}-10^{-2} cm^2 s^{-1}$ and a line extending from this intercept through the doping data has a slope in the range of 0.7–1.2 eV (upper shaded region).[48] These values agree well with calculated values of the binding energy of H to dopants relative to the transport level in the range of 0.9 to 1.2 eV.[21,55]

Another means for introducing traps in c-Si (and thereby lowering μ_H) is by introducing H at very high hydrogen concentrations ($>10^{20}$ cm^{-3}). In this case hydrogenated $\{111\}$-oriented platelets, serving as traps for H, are created. Exposure to a high H concentration results in platelet formation in a region increasing from the surface as a function of time.[29,30,56] One can obtain D_{eff} dominated by platelet formation indicated by the large solid circle in Fig. 12.[29] The effective trap depth, or more precisely μ_H pinned by the platelets, is about 1.4–1.5 eV below the transport level in c-Si assuming a $10^{-3}-10^{-2}$-cm^{2}s^{-1} prefactor. The diffusion controlled by these structures falls significantly below that occurring with shallower, dopant related traps. As will be discussed later, the energy of these clustered configurations is expected to be about 1.3–1.5 eV below the c-Si transport level in agreement with our results. Thus, diffusion in c-Si confirms that different traps lead to different D activation energies and similar prefactors.

With this knowledge about H diffusion in c-Si, we can understand features about H diffusion in a-Si. The diffusion in fully hydrogenated a-Si:H from intrinsic to 10^{-2}-cm^{-3} B-doped material shows an intercept $D_{micro}=10^{-2}$ cm^{2}s^{-1} a value remarkably similar to c-Si (solid squares and lower shaded region).[1–3,12,42] Diffusion in 10^{-2}-cm B-doped material is three orders of magnitude higher than undoped a-Si:H but also exhibits a similar intercept.[42,43] The fact that the intercept is quite similar for both c-Si and a-Si confirms our assumptions that the prefactor is approximately constant independent of the material and supports the idea that trap depths can be determined by assuming a prefactor. The simplest explanation for the constant prefactor is that diffusion at the transport level is similar between a-Si and c-Si because the energy of the interstitial H atom is primarily sensitive only to the nearest-neighbor Si atoms. Since the local environment is the same on average, one would ex-

FIG. 12. The diffusion coefficient vs $1000/T$ for a variety of measurements in c-Si and a-Si (crosses, c-Si high-T or low-H concentration, Ref. 54; triangles, doped c-Si, Ref. 48; squares, hydrogenated a-Si:H, Refs. 1–3 and 42; circles, H-depleted a-Si, this study). The large dot is H platelet dominated diffusion in c-Si from Ref. 29. The arrow pointing down indicates the limits placed on deep-trap dominated diffusion from this study. The energies represent the slopes of the various lines and the shaded areas indicate the ranges of values observed.

pect that the transport energies in the bulk are similar. Thus, as for the case of an electron with the minimum metallic conductivity for electrons, the microscopic transport of H at the saddle points is also rather independent of the film properties for Si.

Having demonstrated that D versus $1/kT$ plots identify changes in controlling traps and their activation energies, consider the posthydrogenation results. The slow diffusion (arrow in Fig. 12) derived from the attenuated deuteration experiments (Fig. 6) is clearly on a different lines than other a-Si curves consistent with deep-trap diffusion controlled by dangling bonds. D_{eff} for high H concentrations in the posthydrogenated samples (solid circles) in Fig. 12 is consistent with D_{eff} observed in as-deposited a-Si:H (squares). This observation confirms results that the controlling shallow traps are roughly 1.3–1.5 eV below the transport level. More importantly, these results indicate that diffusion through H-depleted samples with filled deep traps is indistinguishable from as-deposited a-Si:H. The most elementary explanation is that the shallow traps (1.3–1.5 eV) in hydrogenated a-Si and as deposited a-Si:H are similar. A final important observation is that these shallow traps have a similar energy and effect on transport as the H platelets in c-Si indicated by the large circle. Thus, the position of μ_H in a-Si is similar to that observed in c-Si at high H concentrations when it is controlled by platelet formation.

The simple explanation for the data is that the controlling H transport energy states at high concentrations are similar in a-Si and c-Si. Due to the high H concentrations in a-Si:H, μ_H is determined by platelet structures similar to those dominating diffusion for high H concentrations in c-Si. When μ_H drops below the dangling-bond level such as in Fig. 6 indicated by the arrow in Fig. 12, D_{eff} and μ_H become controlled by dangling-bond levels which are at least 1.9 eV below the transport level and could be up to 2.5 eV below. This result we believe is of fundamental importance to understanding H diffusion in all forms of Si: at high concentrations multi-H complexes form the dominant structure in both a-Si and c-Si.[20,23] Thus, in high concentrations, multi-H platelets control the diffusion activation energy and trapping kinetics. The implications of multi-H complex formation are essential for further elucidation of the microscopic basis of H diffusion in a-Si discussed next.

C. Microscopic models for H transport in a-Si

Thus far in our discussion we have determined that the H trapping states can be divided into deep traps of low concentration and a larger concentration of shallow traps distributed in energy relative to the transport level. In this section, we would like to discuss possible microscopic models for the various H traps discussed in the previous sections and develop a tentative picture of the H density of states and how H moves through a-Si. While the exact microscopic situation cannot be uniquely determined, we believe that on the basis of our data in the previous sections and published theoretical and experimental data, the possibilities can be limited to two general models. In the following section, we will present data which

attempt to distinguish between the two possibilities and discuss the implications of the models for the structure of a-Si:H.

Since we have some idea of the experimental energies for the deep and shallow traps, it is worthwhile to compare these energies to the known theoretical ranges of energies for H bonding in Si.[21,26,27] A summary of these energies for c-Si is shown in Fig. 13(b) in terms of energy/H relative to atomic H in vacuum. Many of these energies have been tested against experiments such as H solubility, chemical dissociation data, etc. Disorder in a-Si will broaden single levels into ranges but the average energy should not change significantly. From the relationship to ESR spins, we conclude that at least a large fraction of deep traps are associated with dangling bonds, Si-H bonds when occupied. These states are at -3 to -3.4 eV/H. Consequently, we know that the transport barrier is at least about 1.9 eV above this energy with the two extreme possible energies indicated by the shaded regions in Figs. 13(a) and 13(c).

1. Platelet or closed void model

In case (a) or the platelet model,[57] the transport is assumed to be similar to the level occurring in c-Si, namely, at about -0.5 eV/H. Thus, H engaged in long-distance transport encounters at least one approximately normal Si barrier during its motion. In this model, the $(1-10)\times10^{21}$ cm^{-3} shallow H states controlling diffusion are in the range of about -2 eV/H. The H
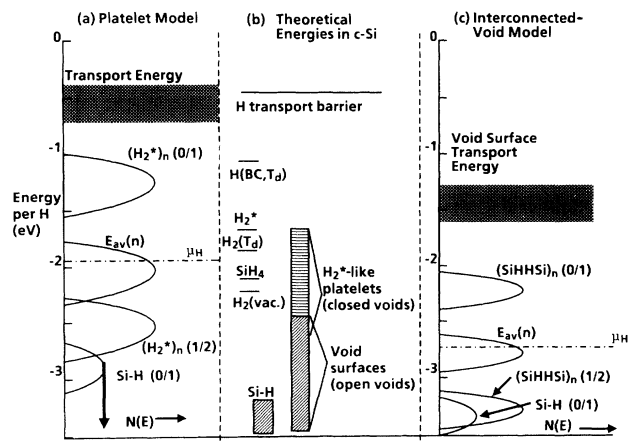

FIG. 13. Diffusion density of states for the platelet model (a) and the hydrogenated void model (c) showing the energy ranges of transport (shaded region), H complexes and Si-H. The arrows indicate that only an upper bound is determined in this study. In (b) is a summary of the calculated energies for various configurations. The energy scale is the energy per H atom to form the various configurations from bulk c-Si or a surface for the void surfaces and the Si-H configuration. The energy zero is atomic H in vacuum. The location of μ_H from diffusion is indicated by the dash-dotted line. The transitions levels for each member of a pair is denoted with (0/1) and (1/2) while the distribution of states pinning μ_H is denoted by $E_{av}(n)$ where the energy depends on the number of pairs in the cluster.

configurations consistent with this possibility are those consisting of H_2^* platelet structures [Fig. 13(b)]. These multi-H clusters are easily capable of holding the up to 10–15 at. % H present in a-Si:H. As with all such clusters the effective H binding energy depends on the number of H atom n in the cluster. The bigger the cluster the greater the binding energy. A suggestive hypothesis is that the time dependence of the diffusion coefficient may arise from the kinetics of nucleation and growth of large platelets resulting in deeper traps for H. The platelets are equivalent to closed voids in that upon H elimination, the void disappears and is replaced by average strength Si-Si bonds. The opposing sides of the void interact to reconstruct following H elimination. This model is supported by our observation that the platelet dominated diffusion in c-Si lies on a D_{eff} versus $1/kT$ line similar to those found in posthydrogenated and amorphous silicon. The corresponding H densities of states for effective thermodynamic energies $E_{av}(n)$ is important if the clusters can capture and release at least two H atoms during the diffusion experiment. Also shown are transition levels for adding or removing 1 or 2 H atoms, also indicated by $(H_2^*)_n(0/1)$ and $(H_2^*)_n(1/2)$, respectively, which are important for short-time experiments.

2. Interconnected void model

The alternative extreme shown in Fig. 13(c) is that H transport takes place along void surfaces or regions of weak Si-Si bonds at energies around -1.5 eV/H. The corresponding shallow-trap energies are at about -2.8 eV/H and are characteristic of void surfaces. The shallow traps are the surfaces of voids which have a range of sizes and also energies $E_{av}(n)$ and transition levels $(SiHHSi)_n(0/1)$ and $(SiHHSi)_n(1/2)$. $E_{av}(n)$ for these sites is somewhat higher (0.3–0.4 eV/H) than isolated dangling bonds due to the average weak surface reconstruction energy when the H is removed.[27] An example of the latter are adjacent dangling bonds on a Si(100) surface which create Si-Si bonds of energies 2 eV or about 1 eV/H removed. The transport energy in the interconnected void model is about 1 eV lower than in c-Si because the H diffuses along the interconnected void surfaces. In this model the intermediate structure of a-Si:H allows H to move large distances without encountering a normal c-Si barrier, thereby lowering the effective transport level with respect to c-Si. These H structures are termed open voids in that when H is removed, a void remains. There is negligible interaction between opposing sides of the void preventing significant reconstruction.

3. Evidence for the models

The two extreme case models are similar in many ways with the primary differences being the binding energy of the majority of H and the H transport energy. Microscopic structures of the platelets and hydrogenated voids are also similar in some respects. Both are clusters of H and some or all of the voids may be planar in structure. The platelets expand creating interior space, and both are

characterized by Si-H bonds. It is highly likely that the actual case is somewhat between these extremes depending on deposition conditions. There are a number of important differences between platelets and hydrogenated voids which have a number of testable consequences.

(1) Consider the IR absorption spectra. Virtually all hydrogenated surfaces exhibit a Si-H stretching frequency near 2100 cm^{-1}.[6–8] Hence, any hydrogenated void which is larger than the grain boundary spacing in poly-Si should exhibit 2100-cm^{-1} absorption. A platelet with the interacting sides, on the other hand, is expected to have vibration frequencies which differ due to interactions with the opposite side. Hence, void-rich a-Si:H deposited at high deposition rates or low temperatures with density deficits as large as 15% of c-Si will have 2100-cm^{-1} absorption and H diffusion characteristic of interconnected voids.[2,13] Diffusion occurs as H_2 and recent evidence that there is virtually no diffusion in some void-rich samples suggest that the H bonding is dominated by hydrogenated void surfaces in poor material and the traps are so deep as to suppress diffusion.[40] Good quality material is proposed to be dominated by platelet-type H phases without the 2100-cm^{-1} absorption, and the H diffusion is monatomic similar to platelet-dominated diffusion in c-Si (Fig. 13).

(2) Materials with a large number of internal voids trap a relatively large concentration of H_2 molecules upon heating since H_2(vac) is energetically favored—a result observed in μc-Si. In good material H_2 molecules have a reduced tendency to form indicating that platelet structures predominate rather than open voids.[58]

(3) The compressive stress ranging from 200 to 800 MPa observed in a-Si:H (Refs. 59 and 60) is expected if platelets structure dominate since the H pushes the Si network apart. The void-rich material, on the other hand, would be expected to be stress-free or even under tensile stress due to the absence of Si. Platelet-rich material should contract upon H evolution while material with hydrogenated voids would contract less, if at all. This contraction has been observed following H evolution.[2]

(4) For any hydrogenated large scale voids of the order of 0.5-nm radius, the ratio of surface H atoms to missing Si atoms of the void is 2 or less. Hence standard material with 10–12 at. % H would be expected to have a density deficit of 5–6 % if all H resided on void surfaces. This is substantially greater than the 2.7% deficits observed in high-quality films.[61] A significant fraction of H must reside in configurations which have a smaller deficit per H atom such as a plateletlike structure.

(5) Finally, the fact that under some conditions etching of a-Si is observed in the presence of a H_2 plasma while Si growth is observed under the same conditions with SiH$_4$ and H_2 in the plasma suggests that μ_H cannot be far from the SiH$_4$ level.[44,60] Due to recombination of H to form H_2(vac), μ_H at the surface is also unlikely to be too different from the H_2(vac) energy level. μ_H pinned near the isolated dangling bonds is too low—etching would never be observed. Hence, μ_H should be in the -2.0-to -2.25-eV range, putting the transport level near -0.5 to -0.7 eV. A rough idea of the energy location of the
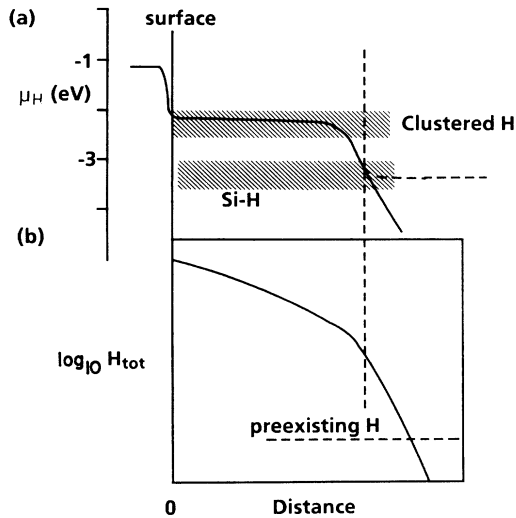
FIG. 14. (a) μ_H as a function of distance from the surface during hydrogenation. (b) represents the corresponding concentration distance. There is a drop in μ_H at or near the surface due to recombination to form H_2 molecules and/or a barrier to penetrating the high hydrogen surface region. At the kink region, μ_H makes a sudden change causing the decrease in diffusion beyond this point. The dashed lines indicate the levels due to preexisting H.

μ_H during the hydrogenation of H-depleted a-Si is shown in Fig. 14. μ_H drops below the defect level when the D concentration is less than the trap level and jumps to the position determined by $E_{av}(n)$ of the clustered phase for higher concentrations. These various arguments presented above suggest that in good quality material, the hydrogen is predominately bonded in plateletlike configurations while in poorer quality material the hydrogen may reside on hydrogenated voidlike structures.

D. Comparison with previous work

Finally, we briefly compare the results of this paper with previous ideas about H bonding in a-Si. The identification of deep traps in H-depleted Si with Si dangling bonds is in good agreement with Ref. 12, where a similar conclusion was determined from H evolution. If there is no H-H exchange interaction our results would suggest that H in 550 °C annealed films is not deeper than about 2.4 eV, while Zellama et al. place the level at about 3 eV. Otherwise H-evolution and H-addition experiments agree about the general details. The weak bound H in Ref. 12 was proposed to be bond-centered H. According to experiments and calculations, this configuration is too mobile, yields gap states, and is not deeply bound. Instead, the weakly bound H is attributed to clustered H in platelet and some hydrogenated void structures. In the cases where the films are highly void ridden, the extreme of the open platelet model, our model for transport would essentially be similar to that proposed by Carlson[62] to explain light-induced defect formation: hydrogen moves along void surfaces.

Our model is an example of the negative-H U-type models investigated by Zafar and Schiff.[16,17] In both

models, the lowest-energy sites are isolated single-H configurations and the higher-energy ones are multi-H configurations. The isolated configurations are separated from the multi-H average energies. The calculations and energies of the negative U model are compatible with the open void extreme, thus we would expect these results to apply for void-rich material. In good material however, we believe that a significant fraction of the defects are due to singly occupied or unpaired H configurations. Otherwise, the 1.5-eV transport activation energy is difficult to understand. Our results are more or less in agreement with the general density of states elaborated in Refs. 15 and 18. The hydrogenated clusters of this work represent a specific microscopic model for the H density of states. From the transport and theoretical results, we know that the dangling bonds are well separated in energy from the multi-H configurations. The H-bonding energies also extend over an energy of about 1.2 eV so there is considerable spread to H-binding energies.

V. SUMMARY

This paper presents preliminary results obtained through the study of H transport in H-depleted amorphous Si. By removing H from a-Si:H, the deepest traps become active traps affecting H transport. The H-diffusion results demonstrate clearly that the density of H configurations can be divided up into deep traps and shallow traps separated in energy. The deep traps are deeper than about 1.9 eV below the transport energy while the shallow traps control the H chemical potential at about 1.5 eV below the transport energy. At least 20–25 % of the deep traps have electron-spin-resonance active dangling bonds indicating that the many of the deepest traps in H-depleted a-Si are associated with dangling bonds. The deep-trap concentration is about $(0.8-2)\times10^{20}$ cm^{-3} and has a capture radius greater than 0.01 nm. The shallower traps are believed to be associated with clustered H phases. There also is a distribution of H-bonding energies rather than a narrow range of energies. The shallow-trap dominated diffusion exhibits dispersion indicating a distribution of trapping and release times, perhaps arising from nucleation and growth kinetics of clustered H. The distribution of release times is consistent with an exponential distribution of barriers with a width of about 0.09 eV (or 1074 K) in rough agreement with previous measurements of dispersive H diffusion. The clustered-phase dominated diffusion in both a-Si and c-Si appear to be identical consistent with the idea that the clustered H phases dominate transport at high-H concentrations exceeding 10^{20} cm^{-3}. The Si network disorder is important only if the H concentration is less than the number of highly strained Si bonds serving as deep traps. Two possible models for H transport are presented which are consistent with the data and calculations. One assumes that in good quality material, the dominant clustered phase of H is platelets or closed voids, characterized by strong interactions between opposite sides of the platelet and net compressive film stress, which form strong Si-Si bonds following H elimination. The dominant H transport occurs at a level similar to that which

occurs in c-Si. In the alternative model, most H resides on the surfaces of interconnected voids which retain their identity following H elimination, have small compressive stress, and are associated with density deficits relative to Si. The H transport in such a model is about 1 eV below its location in c-Si occurring along grain boundaries. Arguments were presented suggesting the possibility that good quality a-Si:H is dominated by the platelet configurations while the open voids dominate the poor quality material.

[1]D. E. Carlson and C. W. Magee, Appl. Phys. Lett. **33**, 81 (1978).

[2]W. Beyer and H. Wagner, J. Non-Cryst. Solids **59&60**, 161 (1983).

[3]M. Reinelt, S. Kalbitzer, and G. Müller, J. Non-Cryst. Solids **59&60**, 169 (1983).

[4]M. H. Brodsky, M. Cardona, and J. J. Cuomo, Phys. Rev. B **16**, 3556 (1977).

[5]G. Lucovsky, R. J. Nemanich, and J. C. Knights, Phys. Rev. B **19**, 2064 (1979).

[6]P. Gupta, V. L. Colvin, and S. M. George, Phys. Rev. B **37**, 8234 (1988).

[7]Y. J. Chabal and K. Raghavachari, Phys. Rev. Lett. **53**, 282 (1984).

[8]H. Richter, J. Trodahl, and M. Cardona, J. Non-Cryst. Solids **59&60**, 181 (1983).

[9]P. C. Taylor, in *Semiconductors and Semimetals, Vol. 21C: Hydrogenated Amorphous Silicon*, edited by J. I. Pankove (Academic, Orlando, 1984), p. 99, and references therein.

[10]J. A. Reimer, R. W. Vaughan, and J. C. Knights, Phys. Rev. Lett. **44**, 193 (1980).

[11]J. B. Boyce and M. Stutzmann, Phys. Rev. Lett. **54**, 562 (1985).

[12]K. Zellama, P. Germain, S. Squelard, B. Bourdon, J. Fontenille, and R. Danielou, Phys. Rev. B **23**, 6648 (1981).

[13]W. Beyer, Non-Cryst. Solids **97&98**, 1027 (1987).

[14]D. K. Biegelsen, R. A. Street, C. C. Tsai, and J. C. Knights, Phys. Rev. B **20**, 4839 (1979).

[15]R. A. Street, M. Hack, and W. B. Jackson, Phys. Rev. B **37**, 4209 (1988).

[16]S. Zafar and E. A. Schiff, Phys. Rev. B **40**, 5235 (1989).

[17]S. Zafar and E. A. Schiff, Phys. Rev. Lett. **66**, 1493 (1991).

[18]R. A. Street, in *Amorphous Silicon Materials and Solar Cells, (Denver, 1991)*, Proceedings of Solutions Needed to Understand and Improve the Light, Soaking Stability of Amorphous Silicon-based Solar Cells, edited by Bryon L. Stafford, AIP Conf. Proc. No. 234 (AIP, New York, 1991), p. 21.

[19]W. B. Jackson, Phys. Rev. B **41**, 10257 (1990).

[20]W. B. Jackson and S. B. Zhang, in *Transport, Correlation and Structural Defects*, edited by H. Fritzsche (World Scientific, Singapore, 1991), p. 63.

[21]C. G. Van de Walle, P. J. Denteneer, Y. Bar-Yam, and S. T. Pantelides, Phys. Rev. B **39**, 10791 (1989).

[22]K. J. Chang and D. J. Chadi, Phys. Rev. B **40**, 11644 (1989).

[23]S. B. Zhang and W. B. Jackson, Phys. Rev. B **43**, 12142 (1991).

[24]R. Jones and G. M. S. Lister, Philos. Mag. B **61**, 881 (1990).

[25]S. B. Zhang, W. B. Jackson, and D. J Chadi, Phys. Rev. Lett. **65**, 2575 (1990).

[26]D. C. Allan, J. D. Joannopoulos, and W. B. Pollard, Phys.

Rev. B **25**, 1065 (1982); **26**, 3475 (1982).

[27]J. Northrup (private communciation); J. E. Northrup and M. L. Cohen, Phys. Rev. Lett. **49**, 1349 (1982); K. C. Pandey, *ibid.* **47**, 1913 (1981).

[28]See *Hydrogen in Silicon: Semiconductors and Semimetals*, edited by J. I. Pankove and N. M. Johnson (Academic, New York, 1991), Vol. 54, and references therein.

[29]N. M. Johnson, D. K. Biegelsen, and M. D. Moyer, Appl. Phys. Lett. **40**, 882 (1982).

[30]N. M. Johnson, C. Doland, F. Ponce, J. Walker, and G. Anderson, Physica B **170**, 3 (1991).

[31]J. Boyce, Physica B **170**, 305 (1991).

[32]A. Chenevas-Paule and A. Bourret, J. Non-Cryst. Solids **59&60**, 233 (1983).

[33]R. Bellissent, in *Amorphous Silicon and Related Materials*, edited by H. Fritzsche (World Scientific, Singapore, 1988), p. 93; R. Bellissent, A. Chenevas-Paule, and M. Roth, J. Non-Cryst. Solids **59&60**, 229 (1983).

[34]P. G. LeComber and W. E. Spear, Phys. Rev. Lett. **25**, 509 (1970).

[35]T. Tiedje, in *The Physics of Hydrogenated Amorphous Silicon II*, edited by J. D. Joannopoulos and G. Lucovsky (Springer-Verlag, Berlin, 1984), p. 261.

[36]J. M. Marshall, J. Berkin, and C. Main, Philos. Mag. B **56**, 641 (1987).

[37]N. M. Johnson, J. Walker, and K. W. Stevens, J. Appl. Phys. **69**, 2631 (1991).

[38]W. B. Jackson, C. C. Tsai, and C. Doland, Philos. Mag. B (to be published).

[39]W. B. Jackson, C. C. Tsai, and R. Thompson, Phys. Rev. Lett. **54**, 56 (1990).

[40]N. Sol, D. Kaplan, D. Dieumegard, and D. Dubreuil, J. Non-Cryst. Solids **35&36**, 291 (1981).

[41]J. Shinar, R. Shinar, S. Mitra, and J.-Y. Kim, Phys. Rev. Lett. **62**, 2001 (1989); X.-M. Tang, J. Weber, Y. Baer, and F. Finger, Solid State Commun. **74**, 171 (1990); Phys. Rev. B **41**, 7945 (1990).

[42]R. A. Street, C. C. Tsai, J. Kakalios, and W. B. Jackson, Philos. Mag. **56**, 305 (1987).

[43]W. Beyer, J. Herion, and H. Wagner, J. Non-Cryst. Solids **114**, 217 (1989).

[44]B. Abeles, L. Yang, D. Leta, and C. Majkrzak, J. Non-Cryst. Solids **97&98**, 353 (1987).

[45]H. Shirai, J. Hanna, and I. Shimizu, Jpn. J. Appl. Phys. **30**, L679 (1991).

[46]R. Street, Phys. Rev. B **43**, 2454 (1991).

[47]T. R. Waite, Phys. Rev. **107**, 463 (1957).

[48]C. Herring and N. M. Johnson, in *Hydrogen in Silicon: Semiconductors and Semimetals* (Ref. 28), Chap. 10.

[49]S. J. Pearton, J. W. Corbett, and T. S. Shi, Appl. Phys. A **43**,

153 (1987).

[50]S. Coffa, J. M. Poate, D. C. Jacobson, W. Frank, and W. Gustin (unpublished); S. Coffa and J. M. Poate (unpublished).

[51]M. Nakamura, T. Ohno, K. Miyata, N. Konishi, and T. Suzuki, J. Appl. Phys. **65**, 3061 (1989).

[52]J. M. Marshall, R. A. Street, and M. J. Thompson, Philos. Mag. B **54**, 51 (1986).

[53]W. Beyer and H. Overhof, in *Semiconductors and Semimetals, Vol. 21C: Hydrogenated Amorphous Silicon* (Ref. 9), p. 257.

[54]C. H. Seager, R. A. Anderson, and J. K. G. Panitz, J. Mater. Res. **2**, 96 (1987); A. Van Wieringen and N. Warmholtz, Physics **22**, 849 (1956).

[55]P. J. H. Denteneer, C. G. Van de Walle, and S. T. Pantelides, Phys. Rev. B **39**, 10 809 (1989).

[56]N. M. Johnson, F. A. Ponce, R. A. Street, and R. J. Nemanich, Phys. Rev. B **35**, 4166 (1987).

[57]W. B. Jackson, S. B. Zhang, C. C. Tsai, and C. Doland, in *Amorphous Silicon Materials and Solar Cells* (Ref. 18), p. 37.

[58]J. B. Boyce, S. E. Ready, M. Stutzmann, and R. E. Norberg, J. Non-Cryst. Solids **114**, 211 (1989).

[59]J. P. Harbison, J. Non-Cryst. Solids **66**, 87 (1984).

[60]G. Nakamura, K. Sato, T. Itagaki, T. Ishihara, M. Usui, K. Okaniwa, H. Sasaki, and Y. Yukimoto, J. Non-Cryst. Solids **77&78**, 1469 (1985).

[61]H. Fritzsche, M. Tanielian, C. C. Tsai, and P. J. Gaczi, J. Appl. Phys. **50**, 3366 (1979).
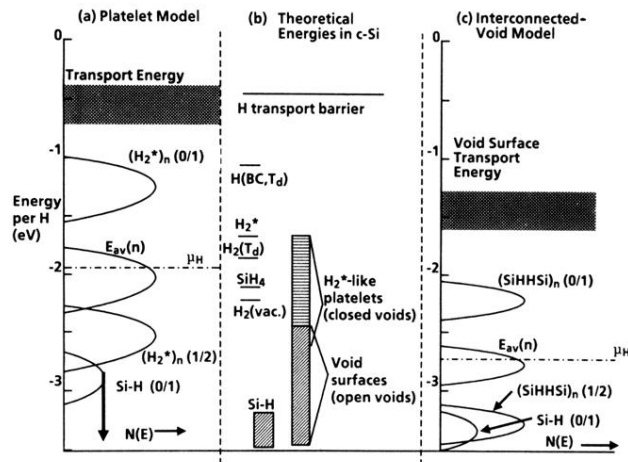
[62]D. E. Carlson, Appl. Phys. A **41**, 305 (1986).

FIG. 13. Diffusion density of states for the platelet model (a) and the hydrogenated void model (c) showing the energy ranges of transport (shaded region), H complexes and Si-H. The arrows indicate that only an upper bound is determined in this study. In (b) is a summary of the calculated energies for various configurations. The energy scale is the energy per H atom to form the various configurations from bulk c-Si or a surface for the void surfaces and the Si-H configuration. The energy zero is atomic H in vacuum. The location of μ_H from diffusion is indicated by the dash-dotted line. The transitions levels for each member of a pair is denoted with (0/1) and (1/2) while the distribution of states pinning μ_H is denoted by $E_{av}(n)$ where the energy depends on the number of pairs in the cluster.